

# Influence of the air humidity on the measurement data acquired with a correlation gas analyzer on the methane and ethane concentration

S.F. Balandin and S.A. Shishigin

*Institute of Atmospheric Optics,  
Siberian Branch of the Russian Academy of Sciences, Tomsk*

Received March 31, 2006

We analyze the performance of modern instrumental complexes intended for remote detection of local methane anomalies in the air. We have developed an IR correlation methane gas-analyzer. Its specifications are presented in this paper. The correlation coefficients calculated at different air humidity are presented.

## Introduction

The real-time monitoring of the methane concentration in air is now the task of the extreme urgency. It could provide for timely warning about technogenic disasters at oil and gas pipelines, in mines and in the industrial premises. This job is being done with the use of contact and remote devices.<sup>1-4</sup> Gas analyzers that use air sampling from the air volume surveyed employ semiconductor, thermocatalytic, electrochemical, spectral-optical, and flame-indication sensors. The type of the instrument is selected based on of such performance characteristics as its selectivity to the gas measured, sensitivity threshold, reliability, design simplicity, maintenance requirements, and cost. The methane detection threshold is about  $2 \text{ ng/m}^3$  (Ref. 1). The threshold concentration sensitivity for methane in air is lower than 0.04 ppm (Refs. 2 and 12).

The use of contact gas analyzers at hard-to-reach places, where sampling is difficult, is limited. Therefore, in recent years an explicit tendency has been observed toward development of airborne instrumentation for the real-time remote monitoring of methane.<sup>3,4</sup> This significantly improves the efficiency of detection of various methane anomalies on vast territories.

## 1. Analysis of the methane gas analyzers

The existing Russian systems for monitoring of  $\text{CH}_4$  are used in geological survey and geophysical studies at the stage of detection and contouring the promising regions in exploring oil and gas fields. Such systems include contact gas analyzers, for example, Obzor-2, MAG-1, AERPOISK, and DOU, which are installed onboard a helicopter and allow the detection of the methane content in air to be performed in the concentration range from 0.01 to  $0.05\% \cdot \text{m}$  (percentage of the detected gas in the unit volume of the medium multiplied by the optical path length).

The background methane concentration is obtained from analysis of the outboard air samples collected as the helicopter flies over the region surveyed.<sup>4</sup> However, such devices are incapable to detect local leakages of methane at altitudes below  $\sim 4.0 \text{ m}$ , which restricts significantly the field of their application.

Among the gas-analysis systems that are exploited nowadays those intended for remote monitoring (see Table 1) are most promising.<sup>3-7</sup>

Among the promising devices there is, in particular, a DLS-PERGAM remote laser methane detector. Its operating principle is based on scanning the methane absorption band centered at  $1.65 \mu\text{m}$  with the frequency tunable radiation of a diode laser. The intensity of the methane absorption band in this spectral range is 2 to 3 orders of magnitude lower than that in the ranges of  $3.3$  and  $7.8 \mu\text{m}$ , which restricts the use of this spectral range for the lidar sensing of methane only to its high concentrations.<sup>3</sup> The threshold sensitivity of measurements for the time of  $0.5 \text{ s}$  from the distance of  $100 \text{ m}$  is  $100 \text{ ppm} \cdot \text{m}$ , which allows the measurement of the excess over the background concentration. However, the need to tune the frequency of the laser radiation in the range of an absorption line of the gas under study, high requirements to the scattered laser radiation coming to the lidar receiver (obligatory account of the fluctuations of molecular and aerosol extinction for laser radiation along the sounding path and variation of the scattering properties of the reflecting surface during frequency tuning across the absorption line of the gas monitored), difficulty to use, and impossibility of simultaneously detecting other gases in the volume under study restrict the practical application of this lidar in geological survey and research.

The disadvantages mentioned above can be eliminated in the case of remote measurements of a foreign gas in air by a correlation radiometer,<sup>5-8,10,11</sup> operating both in the passive mode, by recording the thermal radiation from the surface or the scattered and direct solar, and in the active mode, by recording

**Table 1. Systems for remote detection of methane leakages**

| System  | Manufacturer                           | Configuration   | Carrier                 | Threshold detection         | Practical application              |
|---|--|---|-------------------------|-----------------------------|------------------------------------|
| SAVR airborne scanning radiometric system         | CETM Ltd., Trekhgornyyi, Russia        | 1. Scanning thermovision system SAVR-M, SAVR-S, and Klimat-S<br>2. Coordinate system  | Helicopter, airplane    | 70–100 m <sup>3</sup> /day  | Model sections of gas pipelines    |
| Laser-thermovision system                         | CIP, Moscow, Russia                    | 1. Thermovision camera<br>2. Agema-1000 thermovision system<br>3. Laser gas analyzer<br>4. Onboard computer<br>5. Coordinate system | Helicopter, car, vessel | 340–350 m <sup>3</sup> /day | Mostransgaz, Permtransgaz, CS, UGS |
| Ridim-gaz radar leakage detection system          | Ulan-Ude Aircraft-Repair Plant, Russia | 1. Kontur-A813C meteorological radar<br>2. Coordinate system  | Car                     | 250–300 m <sup>3</sup> /day | Lentransgaz                        |
| Gas Finder 2.0 system                             | –                                      | 1. Diode laser<br>2. Retroreflectors<br>3. Transmitter/receiver system  | Helicopter              | 1 ppm                       | Permtransgaz                       |
| System for remote monitoring of ecological safety | NIKI OEP, Sosnovyi Bor, Russia         | 1. Vezuvii-EK lidar system<br>2. Coordinate system  | Helicopter, airplane    | 200 m <sup>3</sup> /day     | Under development                  |
| DLS-PERGAM methane detector                       | PERGAM Engineering, Moscow, Russia     | 1. Optical system<br>2. Coordinate system   | Helicopter              | 1 ppm                       | –                                  |

the radiation, having passed along the sounding path from an artificial source set at the beginning or at the end of the path. In this case, the methane origin can be identified with the aid of additional measurements of another gas, e.g., ethane, which is also a component of the natural gas mixture, on the same path and by the same device.<sup>5</sup>

According to literature,<sup>5</sup> the sensitivity of  $7 \cdot 10^{-3} \% \cdot \text{m}$  is achieved in the measurements of the methane content in air in the  $7.8 \mu\text{m}$  range by a correlation gas analyzer. To record the background methane concentration (1.6 ppm), a path no shorter than 50 m is needed. In this spectral range, the methane absorption band overlaps with a water vapor absorption band.

In this paper, using the IAO SB RAS databank on spectral lines of atmospheric gases, the influence of the air humidity on the measurement data acquired with a correlation radiometer has been studied for the first time at the variable width of the analyzed spectral range; the estimated performance parameters of the proposed construction of a passive correlation gas analyzer for methane and ethane detection are presented.

## 2. Principle of operation of a correlation radiometer

Using the gas filter correlation method, the frequency spectrum of the radiation absorbed or emitted by the gas to be detected is separated out by the highly efficient and highly selective spectral filter, which is a sample of this gas itself placed in the first channel the signal from which is compared with the reference signal generated in the second channel. The gas concentration in the volume studied is judged from the shift of balance between the data in the two channels. The optical thickness of the gas in the correlation cell (within a selected spectral

region) is chosen so that the product of the modulation depth of the input light flux by the average transmission coefficient reaches its maximum.

The difference signal  $\delta\Phi$  between the two channels is proportional to the total amount of the gas in the air column along the path within the cone, limited by the telescope field of view, and can be expressed as follows<sup>5</sup>:

$$\delta\Phi = A\Omega \int_{\delta v} [\eta_c N_T(v) \exp(-\tau_c(v)) - \eta_r N_T(v) \exp(-\tau_r(v))] dv + I_c, \quad (1)$$

where  $\eta_c$  and  $\eta_r$  are the transmission coefficients for the optical signal components in the correlation and the reference channels;  $A\Omega$  is the angular acceptance;  $\tau_c(v)$  and  $\tau_r(v)$  are the optical thicknesses of the gases in the correlation and reference cells;  $I_c$  is the term corresponding to the radiation emitted by the gas in the correlation cell;  $N_T(v)$  is the total energy brightness of the Earth's surface and the atmosphere within the telescope field of view. According to a simplified model of a homogeneous single-layer atmosphere we have that

$$N_T(v) = [\varepsilon(v) B_e(v, \Theta_e) \exp(-\tau_a(v)) + B_a(v, \Theta_a) (1 - \exp(\tau_a(v)))] \quad (2)$$

where  $B_e(v, \Theta)$  is the brightness, at the frequency  $v$ , of the black body at a temperature  $\Theta$ ;  $\varepsilon$  is the relative emittance (emissivity factor) of the earth's surface, and  $\tau_a(v)$  is the optical thickness of the gas sought. The subscript "e" corresponds to the Earth, while the subscript "a" corresponds to the atmosphere.

The accurate balance between the signals from the correlation and reference cells is needed for the difference signal  $\delta\Phi$  to be independent of variations

in the source brightness in the absence of the gas sought.

With the account of Eq. (2) and the balance, equation for  $\delta\Phi$  (1) can be written as follows:

$$\delta\Phi = A\Omega\eta_c(\epsilon B_e - B_a) \left( \int_{\delta\nu} T_a T_c d\nu - 1/\delta\nu \int_{\delta\nu} T_a d\nu \int_{\delta\nu} T_c d\nu \right) + I_c. \quad (3)$$

It is assumed here that the spectral sensitivity in the reference channel is constant over the working frequency range, and the designation  $T(\nu)$  is introduced for the transmission coefficient  $T(\nu) = \exp(-\tau(\nu))$ .

In practice, the balance condition is controlled by changing the amplification of the signals corresponding to the correlation and reference cells. The amplification is regulated so that the amplified signals are equal in the absence of the sought gas. The parameter

$$\rho_n = \left( \int_{\delta\nu} T_a T_c d\nu - 1/\delta\nu \int_{\delta\nu} T_a d\nu \int_{\delta\nu} T_c d\nu \right)$$

is called the non-normalized correlation coefficient, determining the operation principle of any correlation spectrum analyzer. The maximum sensitivity of the device is achieved through the optimization of the product  $\eta_c$  by  $\rho_n$ . It follows from the equation obtained that the optimal optical thickness of the correlation cell depends on the detailed structure of the spectrum of the gas studied.

Taking into account that the normalized correlation coefficient  $\rho$  between  $T_c(\nu)$  and  $T_a(\nu)$  can be written in the form

$$\rho = \left( \int_{\delta\nu} T_a T_c d\nu - 1/\delta\nu \int_{\delta\nu} T_a d\nu \int_{\delta\nu} T_c d\nu \right) / \sigma_{T_c} \sigma_{T_a}, \quad (4)$$

where  $\sigma_{T_c}$ ,  $\sigma_{T_a}$  are rms deviations of the functions  $T_c(\nu)$  and  $T_a(\nu)$  in the spectral range  $\delta\nu$ , we obtain the functional relationship between the ratio  $\Gamma$  ( $\Gamma = \delta\Phi/\Delta\Phi$ , where  $\delta\Phi$  is the shift of the balance between the channels;  $\Delta\Phi$  is the sum of the signals in the channels) and the correlation coefficient  $\rho$  in the form

$$\Gamma = \rho \sigma_{T_c} \sigma_{T_a} \left[ 2 \int_{\delta\nu} T_a T_c d\nu - \rho \sigma_{T_c} \sigma_{T_a} \right]^{-1}. \quad (5)$$

The dependence of the instrumental function  $\Gamma$  on the correlation coefficient  $\rho$ , which is caused by the parameters of the ambient medium studied (humidity, temperature, pressure, content of other gases), is nonlinear (5). The water vapor content in air varies from  $10^{-3}$  to 8% (tropics).<sup>9</sup>

Figure 1 shows the correlation coefficients obtained for the model atmospheric path with the length of 100 m (the atmospheric content of  $O_2$  is 21%,  $N_2$  – 76–78%, and  $CH_4$  – 0–0.2%) at different specific air humidity  $r = 0$ –3% (3% is the maximum

humidity for the mid-latitudes) in the frequency ranges with the wavenumbers  $k = 1250$ – $1350$  ( $\sim 7.7 \mu\text{m}$  range) and  $2900$ – $3100 \text{ cm}^{-1}$  ( $\sim 3.3 \mu\text{m}$ ).

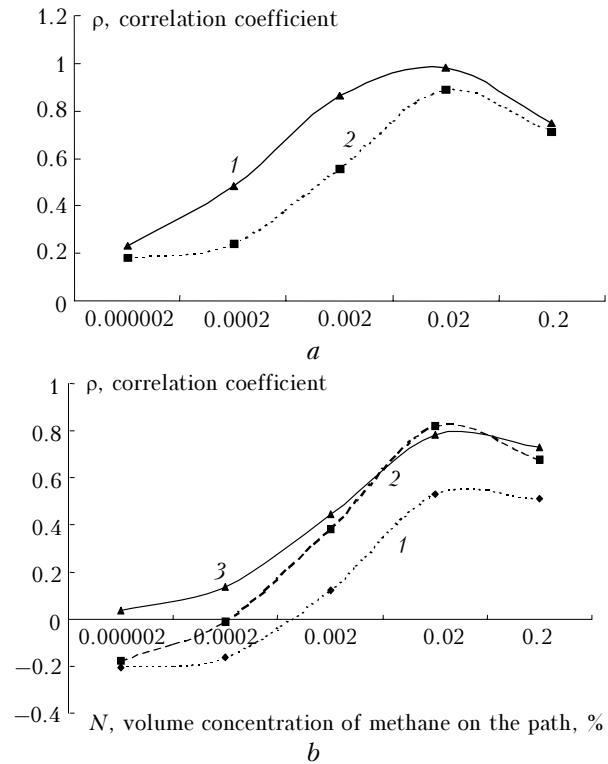


**Fig. 1.** Dependence of the correlation coefficient on the methane concentration:  $k = 1250$ – $1260 \text{ cm}^{-1}$ ,  $r = 0.3$  (curve 1), 3% (curve 2) (a);  $k = 1250$ – $1350 \text{ cm}^{-1}$ ,  $r = 0.3$  (curve 2), 3% (curve 1);  $k = 2900$ – $3100 \text{ cm}^{-1}$ ;  $r = 3\%$  (curve 3) (b).

It can be seen that the correlation coefficient depends on the air humidity, especially, if the width of the analyzed range is chosen equal to the methane fundamental absorption band ( $1250$ – $1350 \text{ cm}^{-1}$ ). This dependence manifests itself in the appearance of the negative values of the correlation coefficient at the low methane content on the path. The signal recorded at the measurement path vanishes at the methane concentration  $N = 2.5$ – $3N_b$ , where  $N_b$  is the background methane concentration in the atmosphere ( $N_b = 1.6 \text{ ppm}$ ), which increases the minimum detectable concentration. To remove this disadvantage and, correspondingly, to improve the threshold sensitivity to the studied gas, we have analyzed the water vapor and methane spectra and separated out the range from  $1250$  to  $1260 \text{ cm}^{-1}$ , in which the overlap between water vapor and methane absorption lines is the least. The calculations have shown that in this spectral range, regardless of the air humidity, the correlation is always positive and the detection threshold can be improved to  $0.5N_b$ .

Because the product of the rms deviations  $\sigma_{T_c}$  and  $\sigma_{T_a}$  of the functions  $T_c(\nu)$  and  $T_a(\nu)$  in this spectral range amounts to thousandth fractions, the difference signal  $\delta\Phi$  (3) also amounts to about  $10^{-3}$  of the signals in each channel.

Thus, the minimal informative signals in each channel should exceed the noise level of the recording system by about three orders of magnitude. This condition determines the minimum power of the radiation coming to the photodetectors of each channel of the radiometer.

The correlation radiometer normally records a spectral range that simultaneously includes tens of spectral lines of the gases studied. Consequently, the source of the radiation analyzed should provide sufficient brightness in the absorption bands of these gases. Artificial thermal sources of radiation (filament lamps, Nernst glower, globar, carbon arc, gas-discharge lamps, etc.), which usually have the emitting surface with the area of no larger than  $1 \text{ cm}^2$ , meet this requirement. Thermal radiation of any surface has, at the temperature of the ambient medium, maximum in the mid-IR spectral region ( $7.5\text{--}12 \text{ }\mu\text{m}$ ). In the case of the lidar (searchlight) sensing, based on recording the radiation scattered back from a remote surface, the power of the backscattered radiation should exceed significantly the power of the thermal radiation of any given surface. If the divergence of the searchlight beam is  $10^{-2} \text{ rad}$ , then the cross section of the light beam is about  $1 \text{ m}^2$  at the distance of  $25 \text{ m}$  from the source.

Table 2 presents the power densities of the black-body radiation  $P$  in the spectral ranges of  $3.3$  and  $7.7 \text{ }\mu\text{m}$  with the width  $\Delta\lambda = 0.03 \text{ }\mu\text{m}$  at the temperatures of  $300$ ,  $2000$ , and  $4000 \text{ K}$ , as well as the estimated area  $S_{\text{source}}$  of the radiation source required at the temperatures of  $2000$  and  $4000 \text{ K}$ . The power of the radiation of this source reflected, in these spectral ranges, from the surface (the reflection coefficient of the surface  $K_{\text{ref}} = 0.05$ ) is equal to the power of the thermal radiation of the black body having the area of  $1 \text{ m}^2$  at the temperature of  $300 \text{ K}$ .

**Table 2**

| $\lambda$ , $\mu\text{m}$ | $\Delta\lambda$ , $\mu\text{m}$ | $T$ , K | $P$ ,<br>$\text{W}/\text{m}^2$ | $K_{\text{ref}}$ | $S_{\text{source}}$ ,<br>$\text{cm}^2$ |      |
|---------------------------|---------------------------------|---------|--------------------------------|------------------|--|------|
| 3.3                       | 0.03                            | 300     | 0.014                          | 0.05             |  |      |
|                           |                                 | 2000    | 3657.82                        |                  |  | 0.77 |
|                           |                                 | 4000    | 14536.55                       |                  |  | 0.19 |
| 7.7                       | 0.03                            | 300     | 0.82                           |                  |  |      |
|                           |                                 | 2000    | 268.55                         |                  |  | 611  |
|                           |                                 | 4000    | 696.98                         |                  |  | 235  |

It can be seen that in the case of the active (lidar) method of measurement of the gas content in the medium studied with a correlation radiometer, it is necessary to have a thermal source with the significantly large emitting area and low beam divergence (to provide for the minimum area of reflection from remote objects). These requirements are difficult to meet even in the spectral range of  $3.3 \text{ }\mu\text{m}$ , to say nothing about the long-wavelength range.

In the IR spectral region, the open-path and passive measurement methods are acceptable for gas analysis using a correlation radiometer. Taking into

account the energy characteristics of the thermal radiation of the Earth's surface and the sources of IR radiation, we assume, based on our calculations, that the methane absorption band at  $3.3 \text{ }\mu\text{m}$  is optimal for the open-path method of methane measurements in the atmosphere, while the band at  $7.8 \text{ }\mu\text{m}$  is most suitable for the passive measurement method. The influence of specific air humidity varying in the range from  $0\text{--}3\%$  on the signal recorded within the spectral range from  $1250$  to  $1350 \text{ cm}^{-1}$  does not exceed  $30\%$  according to Eq. (5), while in the range of  $2900\text{--}3150 \text{ cm}^{-1}$  it is less than  $5\%$ . Isolating the narrow spectral range from  $1250$  to  $1260 \text{ cm}^{-1}$  decreases the influence of humidity on the recorded signal and improves the threshold sensitivity to the gas studied.

The investigations carried out in the range of the ethane absorption band of  $790\text{--}860 \text{ cm}^{-1}$  ( $\sim 12 \text{ }\mu\text{m}$ ) have shown that the influence of the air humidity on the accuracy of measurement of this gas does not exceed  $10\%$ .

### 3. Optical arrangement of the IR radiometer

Based on the obtained results of theoretical investigation of the humidity influence on the threshold sensitivity to the concentration of the studied gas depending on the chosen spectral range, we propose the following optical arrangement of the passive IR radiometer, with the improved threshold sensitivity, for measurements of the methane and ethane on the atmospheric path (Fig. 2).

The IR radiation of the Earth's surface is used as a source of radiation. The radiation is received and selected by a narrow-band selective filter and a specialized cell with the studied gas. Three receiving channels are operated simultaneously: the first channel receives the reference radiation without the gas filter; the second channel detects the radiation with the gas filter for  $\text{CH}_4$ ; the third channel receives the radiation with the gas filter for  $\text{C}_2\text{H}_6$  (ethane). The use of the third channel for ethane allows the unambiguous interpretation of the information obtained and the estimation of the fraction of atmospheric methane of biological origin. In contrast to the instrument from Ref. 5, which employs a single photodetector and conducts consecutive measurements methane and ethane, in our version the measurement time can be reduced to  $10^{-3}\text{--}10^{-4} \text{ s}$ , what allows the real-time measurements to be carried out.

The measurement technique consists in the following. The Earth's thermal radiation is measured in the IR spectral ranges, coinciding with the methane ( $7.8 \text{ }\mu\text{m}$ ) and ethane ( $12 \text{ }\mu\text{m}$ ) absorption bands. The beam, formed by the Cassegrain telescope 12 and IR lenses 7, 20, 28, 39, comes to three different cooled IR photodetectors 21, 30, 42, where it is recorded. In two channels, the radiation passes through the reference cells, containing methane and ethane. All the channels are previously tuned and calibrated on the atmospheric path.

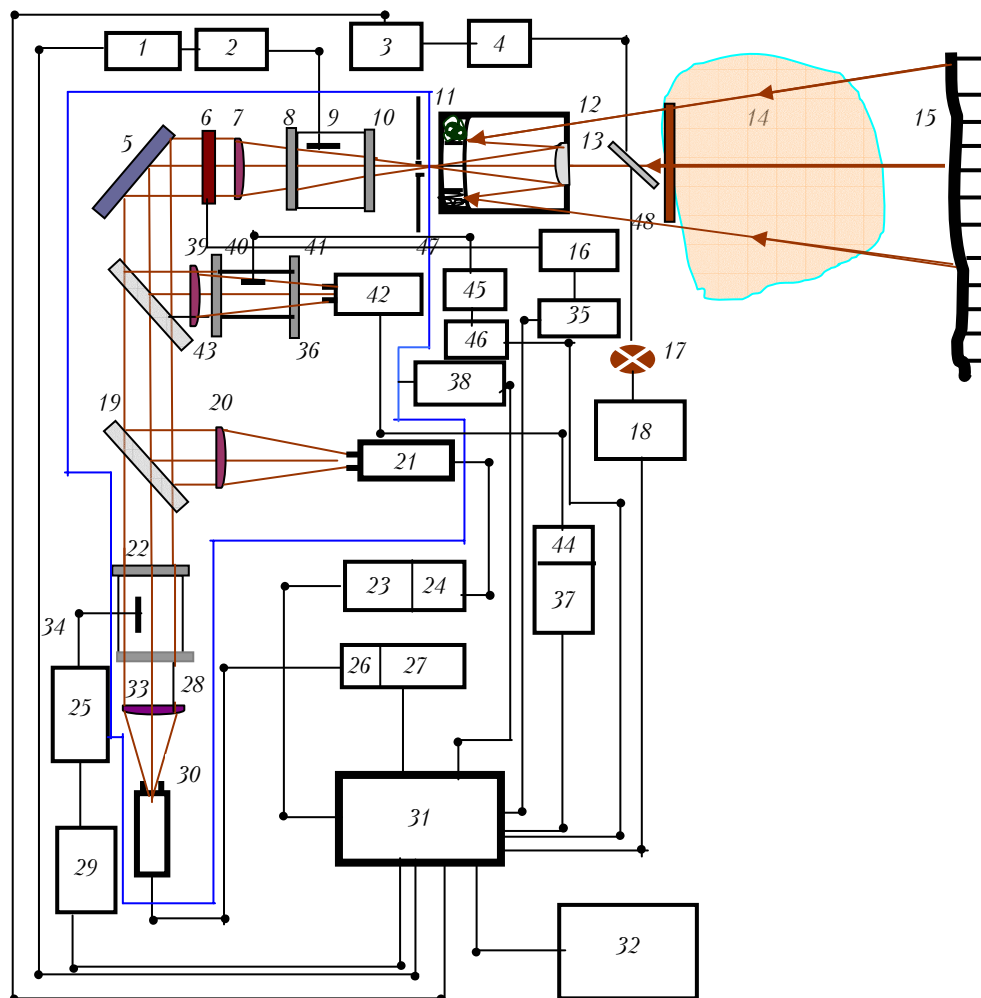


**Fig. 2.** Block-diagram of the correlation IR spectrum analyzer: power supplies of stepper motors 1, 3, 29, 35, 46; stepper motors 2, 4, 16, 25, 45; IR mirrors with nearly 100% reflection 5, 13; turret with bandpass interference filters 6; IR lenses 7, 20, 28, 39; IR windows of quartz cells 8, 10, 22, 33, 40, 41; turret with calibration quartz cells with methane (3 pieces) and ethane (3 pieces) 9; diaphragm 11; Cassegrain IR telescope 12; studied medium 14; surface source of the IR radiation (Earth) 15; calibrating IR radiation source 17; power supply of the calibrating source 18; semitransparent IR plates 19, 43; IR photodetectors 21, 30, 42; amplifiers 24, 26, 44; ADC 23, 27, 37; turrets with reference methane and ethane cells 34, 36; computer 31; computer power supply 32; IR window 48; thermostat 47; thermostat power supply 38.

If there are no studied gases on the path, regardless of the illumination of the Earth's surface, the radiometer readings are zero. In the case of the gas leakage from a pipeline (or other methane sources), a methane cloud with the inhomogeneous distribution of the methane concentration is formed. The additional measurement of ethane, which also is a component of the natural gas, allows the differentiation between methane of natural and biochemical origin.<sup>5</sup> For the measurements of the gas concentrations, the channels are calibrated with the aid of the set of calibration cells in the turret 9 and the calibrated IR radiation source 17. The calibration curves allow the determination of the path-mean concentration of the gases detected.

The main performance parameters of the instrument designed are summarized in Table 3.

**Table 3**

| Parameters of the correlation radiometer  | Methane   | Ethane   |
|---|-----------|----------|
| $\lambda - \lambda + \Delta\lambda$ , $\text{cm}^{-1}$  | 1250–1260 | 790–860  |
| Absorption coefficient, $\text{cm}^{-1} \cdot \text{MPa}^{-1}$  | 1.0       | 1.7      |
| Angular field of view, deg  | 8         | 8        |
| Optical thickness of the gas in the reference cells   | 0.3       | 0.2      |
| Volume content of the measured gas in the correlation cell, %   | 20        | 20       |
| Cell length, cm   | 5         | 5        |
| Photodetector ( $T = 77 \text{ K}$ )  | Hg Cd Te  | Hg Cd Te |
| Detectability of the photodetector $D$ , $10^{10} \text{ cm} \cdot \text{Hz}^{1/2} \cdot \text{W}^{-1}$ | 1         | 1        |
| Threshold sensitivity of the gas analyzer, $\text{ppm} \cdot \text{m}$                                  | 50        | 500      |
| Range of the measured $\text{CH}_4$ concentrations, ppm   | 0.5–20    | 5–200    |
| Measurement error, %  | 15        | 20       |

Thus, in the mid-IR spectral region, the open-path and passive measurement modes are acceptable for the gas analysis by the correlation radiometer. The influence of variations of the absolute humidity on the threshold sensitivity of the radiometer can be decreased considerably if optimally choosing spectral range.

#### 4. Field of application of the correlation radiometer

If produced commercially, the developed scheme of the correlation spectrum analyzer with the improved noise immunity to the humidity can find wide application in the industry and applied research for 1) diagnostics of high- and low-pressure gas pipelines; 2) diagnostics of gas storages, gas tanks, block valve stations, and gas-distribution stations; 3) remote monitoring of the methane concentration near gas leakages; 4) ecological monitoring near industrial plants, gas-distribution stations and other objects; 5) ecological monitoring of natural and agricultural methane sources.

#### References

1. M.T. Dmitriev, N.I. Kaznina, and I.A. Pinigina, *Sanitary-Chemical Analysis of Pollutants in the Environment. Handbook* (Khimiya, Moscow, 1989), 368 pp.
2. V.A. Kapitanov, I.S. Tyryshkin, N.P. Krivolutskii, and Yu.N. Ponomarev, *Atmos. Oceanic Opt.* **17**, No. 8, 553–555 (2004).
3. A.I. Karapuzikov, I.V. Ptashnik, O.A. Romanovskii, O.V. Kharchenko, and I.V. Sherstov, *Atmos. Oceanic Opt.* **12**, No. 4, 350–357 (1999).
4. Yu.M. Andreev, P.P. Geiko, and M.V. Kabanov, in: *Proc. of the Anniversary Scientific-Practical Conf. "Problems and Ways for Efficient Development of Mineral and Raw Resources of Siberia and Far East"* (Tomsk, 2000), pp. 279–282.
5. H.S. Lee and H.H. Zwick, *Prib. dlya Nauch. Issled.*, No. 9, 132–149 (1985).
6. R.M. Richard, *J. Opt. Soc. Am.* **58**, No. 7, 900–908 (1968).
7. T.V. Ward and H.H. Zwick, *Appl. Opt.* **14**, No. 12, 2896–2904 (1975).
8. S.F. Balandin and S.A. Shishigin, in: *Intern. Conf. on Opt. Technol. for Atmos., Ocean, and Environ. Studies (ICOT)* (Beijing, China, 2004), pp. 71–72.
9. V.E. Zuev, *Propagation of Visible and Infrared Radiation in the Atmosphere* (Halsted Press, New York, 1974).
10. B.T. Tolton, *J. Atmos. and Ocean. Technol. Notes and Correspondence* **21**, 837–852 (2004).
11. S.F. Balandin, *Atmos. Oceanic Opt.* **18**, No. 11, 902–909 (2005).
12. V.A. Kapitanov and Yu.N. Ponomarev, *Atmos. Oceanic Opt.* **19**, No. 5, 354–358 (2006).